

Cure Behavior of an Epoxy-Novolac Molding Compound

T. H. HSIEH and A. C. SU*

Institute of Materials Science and Engineering, National Sun Yat-Sen University, Kaohsiung, Taiwan 80424, Republic of China

SYNOPSIS

The isothermal cure of an epoxy–novolac molding compound was studied by means of differential scanning calorimetry (DSC). The glass transition temperature (T_g) of the molding compound increased in an approximately linear manner with conversion (α) during the major part of the cure process. Predictions of an empirical kinetic scheme (established earlier from dynamic DSC results) compared favorably with the present isothermal results in the absence of vitrification. In combination with the gel point conversion (α_{gel}) determined via dynamic rheological analysis and gravimetric measurements, our DSC results indicated that gelation bears no apparent effect on the rate of cure whereas vitrification retards the cure reaction. Based on the measured α_{gel} , the approximate T_g – α relationship, and the thermokinetic results, the time–temperature–transformation diagram of this molding compound was constructed and discussed.

INTRODUCTION

A variety of experimental methods may be used to follow the cure reaction in thermosets. Among them, differential scanning calorimetry (DSC) has been one of the most commonly adopted techniques. As comprehensively reviewed by Prime,¹ the differential scanning calorimeter may be operated under isothermal (i.e., time-sweep) or dynamic (i.e., temperature-scan) modes for the kinetic study of thermosetting systems. However, there are different views in the literature concerning the interpretation of isothermal and dynamic DSC results. Several authors^{2–4} have demonstrated that the kinetic parameters obtained from isothermal and dynamic scans are intrinsically different. An explanation in terms of different curing mechanisms prevailing in different temperature ranges has been offered.^{2–4} Alternatively, Adabbo and Williams⁵ have pointed out that vitrification may induce errors in the evaluation of kinetic parameters from isothermal and dynamic DSC runs. The possibility that gelation may affect the progress of cure reactions has also been suggested⁶: isothermal experiments showed that the reaction rate may slow down from a certain

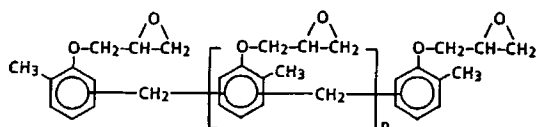
reaction extent located in the rubbery region between the gel point and the glass transition (vitrification) point.^{6–8}

Epoxy–novolac molding compounds have been extensively used in the electronic industry for the encapsulation of integrated circuits by means of transfer molding.^{9,10} However, only limited information concerning the cure characteristics of these molding compounds may be found in the open literature.^{10–13} These molding compounds are mainly composed of silica filler (ca. 70 wt %), an epoxy cresol novolac prepolymer, and a phenol novolac or cresol novolac hardener. The average degree of polymerization of the oligomeric components is typically around 5.¹² The molar ratio between the epoxide and the phenolic hydroxyl groups is commonly in the vicinity of 2.^{10,14} A minor amount of catalyst (typically a Lewis base) is used to accelerate the reaction between the epoxide and the hydroxyl groups.¹⁰ Structures of the component prepolymers and the main reactions involved are given in Figures 1 and 2.

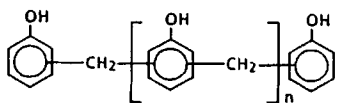
In a previous study,¹⁵ we examined the cure kinetics of a commercial molding compound (Nitto HC-10-2-8) using the dynamic DSC approach. An empirical kinetic expression, i.e.,

$$d\alpha/dt = Af(\alpha)\exp(-E_a/RT), \quad (1)$$

* To whom correspondence should be addressed.



EPOXY CRESOL NOVOLAC



PHENOL NOVOLAC

Figure 1 Structures of the major resin components in typical epoxy-novolac molding compounds.

where $Af(\alpha) = 5.8 \times 10^6 (1 + 4.7\alpha - 6.5\alpha^2) \text{ sec}^{-1}$, $E_a = 18.4 \text{ kcal/mol}$, R is the gas constant, and α is the conversion (or, the extent of cure reaction), has been shown to represent dynamic DSC results in a major conversion range (i.e., up to $\alpha = 0.8$) for widely different heating rates ($\phi = 40\text{--}0.5^\circ\text{C/min}$). We have subsequently directed our attention to the case of isothermal cure at lower temperatures. Along with complementary information provided by a parallel dynamic rheological study, results of our isothermal cure study are reported here. Extensive comparison has been made between results of the present work and those of the previous dynamic DSC study.

EXPERIMENTAL

Material

The molding compound studied was HC-10-2-8 from Nitto Electric Industrial Co. Ltd., Japan. This molding compound is highly filled (ca. 70 wt %) with silica and, according to the supplier, gels within 20 s at 175°C .

Isothermal Cure

In general, DSC methods for isothermal cure studies may be divided into two categories.¹ In the first method, the rate of reaction is continuously monitored in the calorimeter throughout the entire course of isothermal cure; in the second method, the residual heat of reaction evolved in a dynamic DSC scan immediately after isothermal cure of the sample for a given period of time is measured. The equivalency of the two methods has been previously confirmed

by Fava.¹⁶ In the present study, we have chosen to use the second method. Samples approximately 10 mg in weight were enclosed in DSC pans, partially cured in an air-circulating oven for various periods at the cure temperature ($60, 80, \text{ or } 100^\circ\text{C}$), and then removed from the oven and allowed to cool to room temperature before the DSC measurement.

DSC Characterization

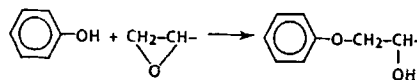
A Du Pont DSC 910 cell connected to a Du Pont 9900 data station was used. The calorimeter was calibrated with an indium standard. Isothermally cured samples contained in DSC pans were scanned in the calorimeter at 10°C/min from ambient temperature to 300°C for the determination of glass transition temperature (T_g) and residual heat of reaction (ΔH_{res}). The total heat of reaction (ΔH_{tot}) and T_g of the as-received molding compound (T_{g0}) was determined by scanning an uncured sample; the T_g at the fully cured state ($T_{g\infty}$) was determined by scanning a postcured (4 h at 180°C under a nitrogen stream) sample.

Typical DSC thermograms obtained for isothermally cured samples are given in Figure 3. In addition to the exothermic peak due to the residual cure reaction, the glass transition may also be observed in the thermogram as shown in Figure 3(a). However, for samples annealed sufficiently long at the cure temperature, the glass transition may develop into an endothermic peak (due to physical aging¹⁷ at the cure temperature) as demonstrated in Figure 3(b). The total area under the cure peak is taken as ΔH_{res} . The extent of cure reaction accomplished during the isothermal cure is then defined as^{1,14}

$$\alpha = (\Delta H_{\text{tot}} - \Delta H_{\text{res}}) / \Delta H_{\text{tot}}. \quad (2)$$

For the sake of consistency, the intersection of the baseline and the tangent drawn through the inflec-

Reaction of the epoxide with the phenolic hydroxyl:



Reaction of the epoxide with secondary aliphatic hydroxyl:

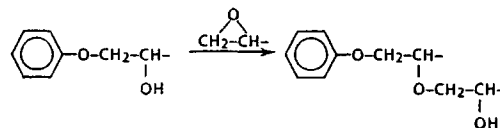


Figure 2 Reactions involved in the cure of typical epoxy-novolac molding compounds.

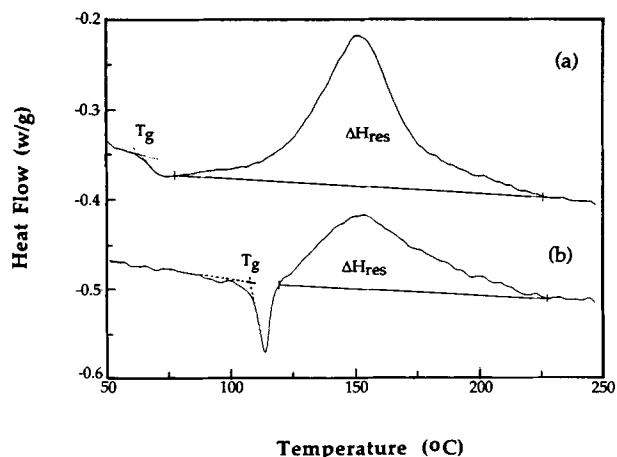


Figure 3 The DSC thermograms of samples cured (a) at 60°C for 12.5 h and (b) at 80°C for 24 h, respectively. Also illustrated is the operational definition of T_g in this work.

tion point of either the sigmoidal glass transition region or the low-temperature side of the physical aging peak is taken as T_g . This may introduce some uncertainties in T_g since the shape and the position of the physical aging peak are known to vary with the aging time.^{18,19} In addition, the physical aging peak may overlap with the cure peak and result in difficulties with the determination of ΔH_{res} (and thus α) for samples in the later stage of the isothermal cure.

Determination of Conversion at Gel Point

Dynamic Rheological Analysis

Dynamic rheological characterization of the molding compound was conducted by use of a Rheometrics RDS-II instrument operated in a frequency range of 1–100 rad/s with a maximum strain of 10%. Cold-pressed discs (ca. 2 mm in thickness) of the molding powder were first heated to ca. 85°C in the parallel-plate assembly for approximately 1 min (to ensure proper “melting” of the sample) before the final adjustment of platen gap to ca. 1.5 mm. Dynamic rheological properties such as storage modulus (G') and loss modulus (G'') were then measured at a given test frequency ($\omega = 1, 10, 50, \text{ or } 100 \text{ rad/s}$) as the chamber temperature was programmed to rise at a nominal heating rate (ϕ) of 5, 10, 20, or 40°C/min. The actual sample temperature was measured through a thermocouple in direct contact with the lower platen. Representative sample temperature histories are given in Figure 4. The temperature–time relationship is clearly nonlinear, i.e., the actual heating rate varies with time and is significantly

lower than the nominal value, especially in the early stage of ramping. Either second-order (for $\phi = 5, 10, \text{ or } 20^\circ\text{C/min}$) or third-order (for $\phi = 40^\circ\text{C/min}$) polynomial regression analysis was thus adopted to represent the sample temperature (T) as a function of time (t) from the start of temperature scan, i.e.,

$$T = \sum c_i t^i, \quad (3)$$

where c_i are fitting coefficients.

Gravimetric Analysis

The as-received molding powder and samples isothermally cured (at 60, 80, or 100°C) in a manner similar to the procedure mentioned earlier were extracted at room temperature in stirred acetone for 3 h. The insoluble portion (which include both the silica filler and the gelled polymer) was vacuum dried (2 h at room temperature and another 3 h at 50°C) and subsequently weighed. Our gravimetric measurements (triplet runs) indicated the presence of $30.0 \pm 0.5 \text{ wt } \%$ resinous components in the as-received molding compound. Consequently, the gel fraction of the partially cured samples were calculated from the gravimetric data according to this initial solubility value.

RESULTS AND DISCUSSION

Extent of Cure at the Gel Point

Given in Figure 5 is an example for the observed variation of G' and G'' with temperature in a typical

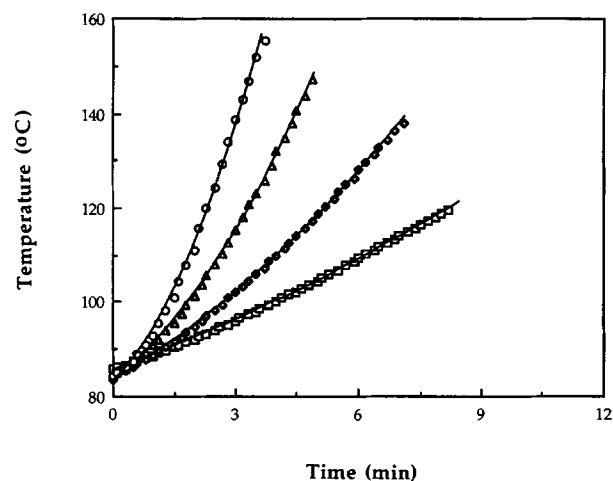


Figure 4 Typical temperature histories in the dynamic rheological characterization of the molding compound: (□), $\phi = 5^\circ\text{C/min}$; (◇), $\phi = 10^\circ\text{C}$; (Δ), $\phi = 20^\circ\text{C}$; (○), $\phi = 40^\circ\text{C}$. The test frequency was 10 rad/s.

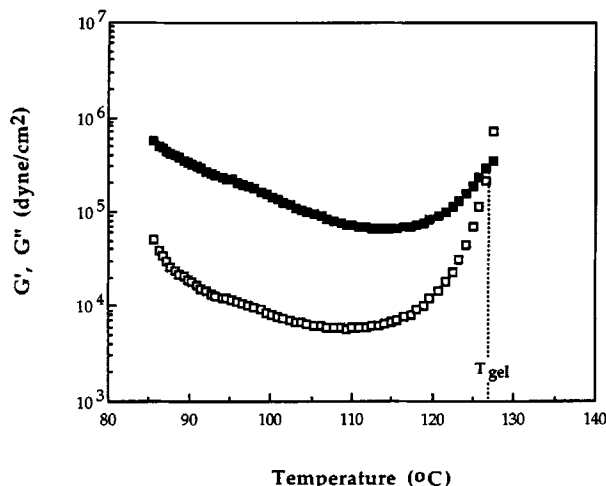


Figure 5 Variation of G' (\square) and G'' (\blacksquare) during the dynamic rheological analysis of the molding compound at $\phi = 5^\circ\text{C}/\text{min}$ and $\omega = 10$ rad/s.

dynamic rheological experiment. The gel point is operationally defined here as the crossover point of the G' and G'' curves as previously proposed by Tung and Dynes.²⁰ The extent of cure at the gel point, α_{gel} , for each sample was then calculated by the use of eqs. (1) and (3). As given in Table I, α_{gel} values lie consistently in the range of 0.14 ± 0.02 although there appears to be a slight tendency for the measured α_{gel} to increase with the heating rate (and therefore the temperature at the G' - G'' crossover)

Table I Conversion and Temperature at the Gel Point in Dynamic Rheological Experiments of Various Nominal Heating Rates and Test Frequencies

ϕ ($^\circ\text{C}/\text{min}$)	ω (rad/s)	T_{gel} ($^\circ\text{C}$)	α_{gel}
5	1	126.5	0.12
	10	127.0	0.12
	50	129.0	0.14
	100	129.0	0.14
10	1	138.0	0.13
	10	137.0	0.12
	50	138.5	0.13
	100	139.5	0.14
20	1	148.5	0.13
	10	148.5	0.13
	50	150.0	0.14
	100	153.5	0.16
40	1	156.5	0.15
	10	156.0	0.13
	50	157.5	0.16
	100	162.0	0.21

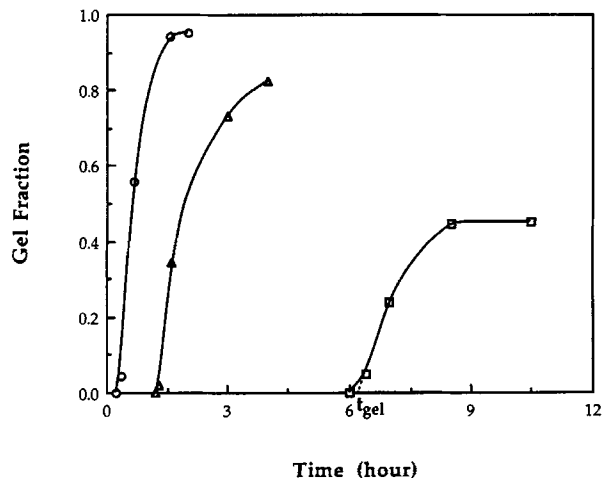


Figure 6 Variation of the gel fraction with time during isothermal cure: (\square), 60°C ; (\triangle), 80°C ; (\circ), 100°C . Also illustrated is the operational definition of t_{gel} .

or frequency. As previously discussed by Winter,²¹ the relationship between the G' - G'' crossover and the true gel point depends significantly on the rheological property of the system at the gel point. The slight heating rate or frequency dependence here may probably be attributed to the possible deviation of G' - G'' crossover from the true gel point.

In addition to the rheological dynamic analysis, the conventional extraction procedure has also been adopted for further access to α_{gel} . Given in Figure 6 are results of the gravimetric analysis. The gel time (t_{gel}) is defined here as the extrapolated initial point of gel formation. At each temperature, the value of α_{gel} was calculated by integrating eq. (1) to the corresponding t_{gel} . Results of our gravimetric measurements indicated that $\alpha_{\text{gel}} = 0.14 \pm 0.01$, in good agreement with that estimated from the dynamic rheological measurements.

Interestingly, a separate dynamic rheological study²² of a similar molding compound resulted in an α_{gel} value of 0.16. The seemingly low value of α_{gel} is not really surprising if the functionality of oligomeric resin components is considered. According to the classical Flory-Stockmayer analysis,²³ the theoretical gel conversion for the present system may be expressed as

$$\alpha_{\text{gel}} = [r(f_e - 1)(f_h - 1)]^{-1/2}, \quad (4)$$

where $r \geq 1$ is the molar ratio of the reacting groups, f_e is the functionality of the epoxy prepolymer, and f_h is the functionality of the novolac prepolymer. For both of the resin components, the degree of polymerization is in the vicinity of 5.¹² Therefore, f_e

$= f_h = \text{ca. } 5$ if the epoxide group is assumed to react exclusively with the phenolic hydroxyl group. The higher reactivity of the epoxide towards the phenolic hydroxyl (as compared to that towards the secondary hydroxyl) is well established; the selectivity, however, depends on the type and the amount of the catalyst used.^{12,24,25} The reaction between the epoxide with the secondary hydroxyl may therefore be ignored temporarily for the sake of simplicity. Based on the assumptions and approximations above, the theoretical α_{gel} value calculated from eq. (4) is 0.18 for the typical epoxide/phenolic hydroxyl molar ratio of 2. This compares favorably with our experimental α_{gel} values; the slight overestimation may understandably be attributed to the neglect of the reactivity of secondary hydroxyls.

Glass Transition: Vitrification during Cure

Given in Figure 7 are representative thermograms for samples isothermally cured for various periods. It is observed that the T_g of an isothermally cured sample increases with cure time and becomes slightly higher than the cure temperature as shown in Figure 8.

Given in Figure 9 are the variation of T_g with α from the present DSC results along with the information of $\alpha_{\text{gel}} = 0.14$ from the gravimetric and the dynamic rheological analyses. Figure 9 is in effect a phase diagram of the molding compound. It may be observed that T_g of the molding compound increases in an approximately linear manner with α during major part of the cure (up to $\alpha = 0.9$) but increases more sharply with α in the final stage. The rela-

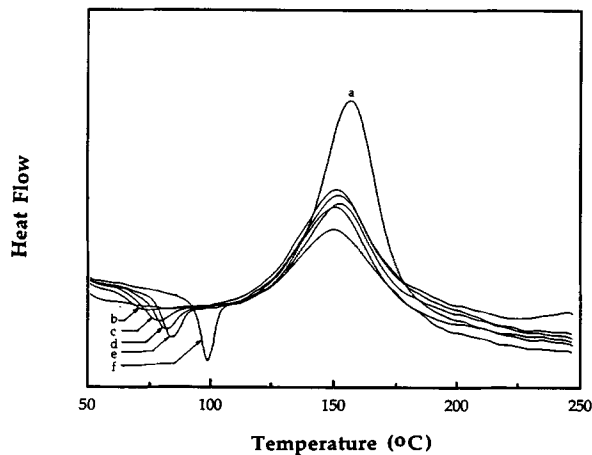


Figure 7 The DSC thermograms for samples cured at 60°C for various times. (a), 1.5 h; (b), 12.5 h; (c), 24.5 h; (d), 47.7 h; (e), 101.2 h; (f), 294 h.

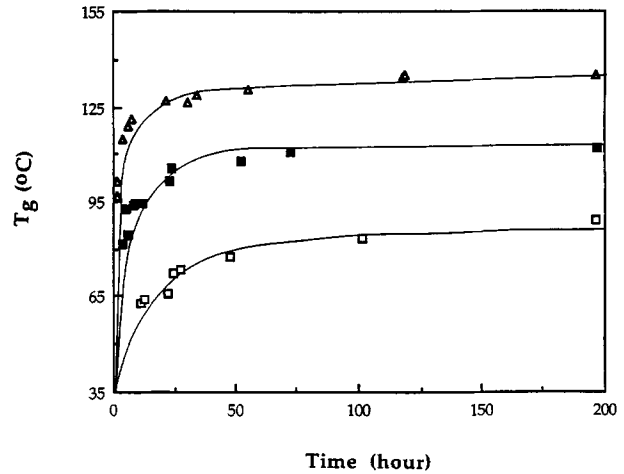


Figure 8 Variation of T_g with time during the isothermal cure: (\square), 60°C; (\blacksquare), 80°C; (\triangle), 100°C.

tionship between α and T_g may be described using the Di Benedetto equation^{26,27}

$$(T_g - T_{go})/T_{go} = \alpha(E_x/E_m - F_x/F_m) / [1 - \alpha(1 - F_x/F_m)], \quad (5)$$

where E_x/E_m is the ratio of lattice energies at cross-linked and uncrosslinked states, F_x/F_m is the corresponding ratio of segmental mobilities, and T_{go} is the glass transition at the uncured state. For the present molding compound, $T_{go} = 35^\circ\text{C}$, T_{goo}

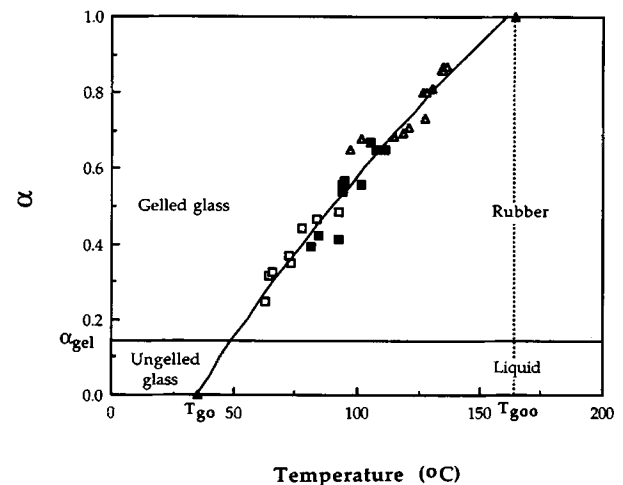


Figure 9 Phase diagram of the molding compound. Symbols correspond to T_g at different conversion levels under isothermal curing at various temperatures: (\square), 60°C; (\blacksquare), 80°C; (\triangle), 100°C. The curve passing through the pack of data points is the best fit to eq. (5); the horizontal line represents the estimated gel conversion.

= 164°C, and the best-fit values of E_x/E_m and F_x/F_m are 1.10 and 0.78, respectively. Experimental E_x/E_m and F_x/F_m values for six epoxy/amine systems have been compiled by Enns and Gillham²⁸; the present results lie among the higher ones of the reported values, reflecting the approximately linear dependence of T_g on α for this molding compound.

Cure Kinetics and Effect of Vitrification

Predictions of eq. (1) for the isothermal cure case are compared with experimental results in Figure 10. It may be observed that the predictions agree fairly well with the experimental results in the early stage of cure. This suggests that, for the present system, isothermal and dynamic experiments share a nearly identical kinetic description in the early stage of cure. However, the predictions are no longer followed in the later stage of the isothermal cure. With the knowledge of positions of gel points (i.e., $\alpha_{gel} = 0.14$) and vitrification points [from eq. (5)], we may now observe that the conversion-time curves do not show significant changes near the gel point and the conversion plateau at each cure temperature is clearly in the close vicinity of the vitrification point. This observation is in strong support to the notion of Adabbo and Williams⁵ that vitrification retards cure reaction. The role of gelation in the present system, however, is not as clear. The agreement between isothermal and dynamic results near the gel point does not necessarily indicate the absence of the effect of gelation on cure reaction because the effect of gelation, if it exists, should have

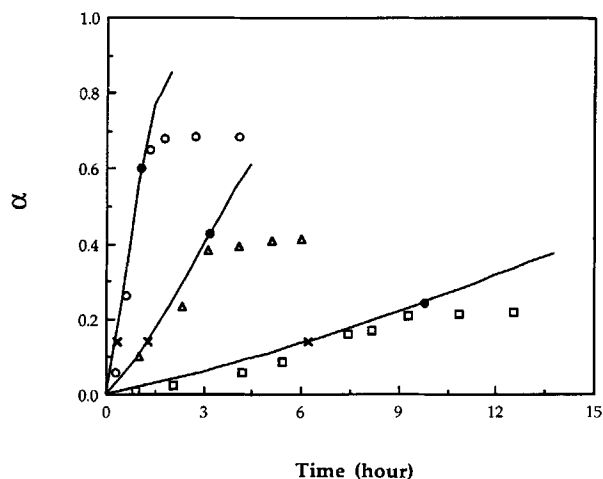


Figure 10 Comparison between results of isothermal cure and predictions from previous kinetic model [eq. (1)]. (—), predictions of eq. (1); (□), (Δ), and (○), isothermal results at 60, 80, and 100°C, respectively; (x) gel point; (●), vitrification point.

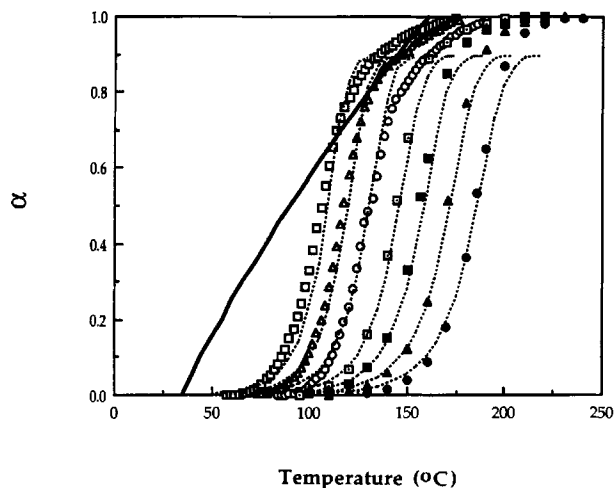


Figure 11 Conversion-temperature trajectories for the dynamic cure of the molding compound. The full line is the T_g - α relationship [eq. (5)]. Symbols are experimental results at different heating rates: (●), $\phi = 40^\circ\text{C}/\text{min}$; (▲), $\phi = 20^\circ\text{C}/\text{min}$; (■), $\phi = 10^\circ\text{C}/\text{min}$; (□), $\phi = 5^\circ\text{C}/\text{min}$; (○), $\phi = 2^\circ\text{C}/\text{min}$; (Δ), $\phi = 1^\circ\text{C}/\text{min}$; (□), $\phi = 0.5^\circ\text{C}/\text{min}$. Corresponding dotted lines are predictions from eq. (1).

already been included in our purely empirical kinetic expression. However, the absence of drastic changes near the gel point does suggest that the effect of gelation, if it exists, is not strong enough to result in any apparent retardation in the rate of cure for the present system.

Given in Figure 11 are some results from a previous dynamic DSC study.¹⁵ In the case of higher heating rates, the empirical kinetic expression [eq. (1)] tends to underestimate the extent of cure in the high conversion region. For lower heating rates, however, this tendency becomes partly reversed and the curves appear suppressed in the higher conversion range. As may be observed, this region of lower-than-expected reaction rate in the low heating rate curves is in the vicinity of the vitrification line given by eq. (5). The apparent overestimation of eq. (1) in this region is therefore attributed to the interfering effect of vitrification. This means that, in dynamic cure experiments of comparatively low heating rates, T_g of the system may catch up with the system temperature (i.e., vitrification may be approached) during the course of cure and result in an apparent slowing down of the cure reaction.

Time-Temperature-Transformation Diagram

Being able to attribute differences in isothermal and dynamic DSC results to the frozen-in effect of vitrification, we are now assured that the single em-

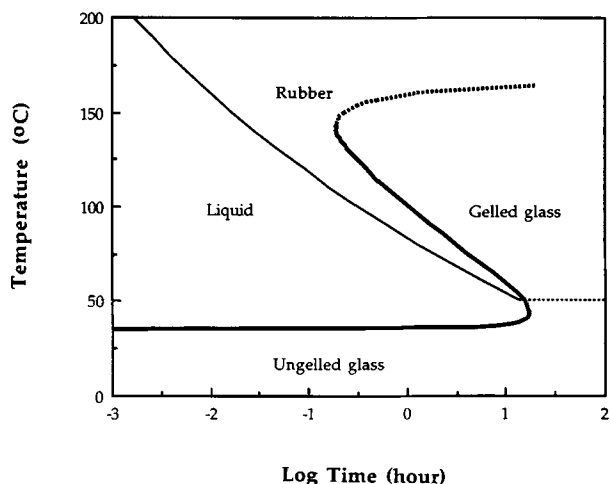


Figure 12 The time-temperature-transformation (TTT) diagram for the present molding compound.

empirical rate expression of eq. (1) may reasonably approximate the kinetic behavior of the molding compound in a wide temperature range. As previously suggested by Ozawa,²⁹ the time to gel and the time to vitrify (t_{glass}) at a given temperature may be obtained by integration of the rate expression [i.e., eq. (1)] from $\alpha = 0$ to α_{gel} (i.e., 0.14) and to α_{glass} [from eq. (5)], respectively. The time-temperature-transformation diagram for this molding compound, as given in Figure 12, may thus be constructed after a series of calculations for different cure temperatures.

In actual practice, preforms of the molding compound are first heated dielectrically to ca. 85°C and then transfer molded at a mold temperature of ca. 175°C. The selection of these conditions may now be rationalized readily from Figure 9 and 12: A pre-heat temperature of ca. 85°C allows for adequate softening (i.e., some 50°C above T_{g0}) of the molding compound yet with a very low cure rate to eliminate changes in properties during handling; a mold temperature of ca. 175°C (i.e., more than 100°C above T_{g0} and slightly above T_{g00}) allows for the combination of good flow and proper cure rate, as well as the minimization of vitrification effect during molding.

CONCLUSIONS

In comparison with our previous dynamic DSC results,¹⁵ the present results for the isothermal cure of the HC-10-2-8 molding compound indicate that the empirical kinetic scheme established earlier is

valid in both the dynamic and the isothermal cases unless the effect of vitrification sets in. Combined results from the earlier and the present studies lend strong support to the suggestion by Adabbo and Williams⁵ that apparent retardation of cure reaction may exist in isothermal as well as in dynamic cases. On the other hand, an earlier proposal⁶ that cure kinetics may be altered near gelation due to the corresponding increase in viscosity (and therefore the transition to diffusion-controlled mechanism) is not confirmed in the present study. The present thermokinetic results will be compared further with additional Fourier-transform infrared spectroscopic and dielectric observations for the cure of this molding compound in a future report.

This work is supported in part by Philips Electrical Building Elements Industry, Inc. (PEBEI). Helpful suggestions in the extraction procedure from Mr. J. C. Hsu of PEBEI are gratefully acknowledged. Thanks are also due to Dr. F. S. Yang and Mr. F. S. Liao of China Steel Corporation for the help T.H.H. received with the RDS-II experiments.

REFERENCES

1. R. B. Prime, in *Thermal Characterization of Polymeric Materials*, E. A. Turi, ed., Academic Press, New York, 1981.
2. R. B. Prime, *Polym. Eng. Sci.*, **13**, 365 (1973).
3. T. Ozawa, *J. Therm. Anal.*, **9**, 369 (1976).
4. A. M. Joven and C. C. Foun, *J. Appl. Polym. Sci.*, **32**, 3761 (1986).
5. H. E. Adabbo and R. J. J. Williams, *J. Appl. Polym. Sci.*, **27**, 1327 (1982).
6. C. C. Riccardi, H. E. Adabbo, and R. J. J. Williams, *J. Appl. Polym. Sci.*, **29**, 2481 (1984).
7. S. Lunak and K. Dusek, *J. Polym. Sci., Polym. Symp. Ed.*, **53**, 45 (1976).
8. K. Horie, H. Hiura, M. Sawada, I. Mita, and H. Kambe, *J. Polym. Sci. A-1*, **8**, 1357 (1970).
9. K. M. Striny, in *VLSI Technology*, 2nd ed., S. M. Sze, ed., McGraw-Hill, New York, 1988.
10. N. Kinjo, M. Ogata, K. Nishi, and A. Kaneda, *Adv. Polym. Sci.*, **88**, 1 (1989).
11. D. J. Belton and M. Molter, *Polym. Eng. Sci.*, **28**, 189 (1988).
12. A. Hale, C. W. Macosko, and H. E. Bair, *J. Appl. Polym. Sci.*, **38**, 1253 (1989).
13. S. Matsuoka, S. Quan, H. E. Bair, and D. J. Boyle, *Macromolecules*, **22**, 4093 (1989).
14. D. B. Fritz and C. S. Wang, in *Polymeric Materials for Electronics Packaging and Interconnections*, J. H.

- Lupinski and R. S. Moore, eds., American Chemistry Society, Washington, DC, 1989, chap. 33.
15. T. H. Hsieh and A. C. Su, *J. Appl. Polym. Sci.*, **41**, 1271 (1990).
 16. R. A. Fava, *Polymer*, **9**, 137 (1968).
 17. L. C. E. Struik, *Physical Aging in Amorphous Polymers and Other Materials*, Elsevier, Amsterdam, 1978.
 18. R. J. Roe and G. M. Millman, *Polym. Eng. Sci.*, **23**, 318 (1983).
 19. D. J. Plazek and Z. N. Frund, Jr., *J. Polym. Sci., Polym. Phys. Ed.*, **28**, 431 (1990).
 20. C. Y. M. Tung and P. J. Dynes, *J. Appl. Polym. Sci.*, **27**, 569 (1982).
 21. H. H. Winter, *Polym. Eng. Sci.*, **27**, 1698 (1987).
 22. F. Lim, *J. Appl. Polym. Sci.*, to appear.
 23. G. Odian, *Principles of Polymerization*, 2nd ed., Wiley, New York, 1981.
 24. F. B. Alvey, *J. Appl. Polym. Sci.*, **13**, 1473 (1969).
 25. P. N. Son and C. D. Weber, *J. Appl. Polym. Sci.*, **17**, 2415 (1973).
 26. L. E. Nielsen, *J. Macromol. Sci., Rev. Macromol. Chem.*, **C3**, 69 (1969).
 27. J. K. Gillham, *Developments in Polymer Characterisation—4*, Applied Science, London, 1982.
 28. J. B. Enns and J. K. Gillham, *J. Appl. Polym. Sci.*, **28**, 2567 (1983).
 29. T. Ozawa, *J. Therm. Anal.*, **2**, 301 (1970).

Received August 25, 1990

Accepted January 31, 1991